using Grouped Zprojector on ImageJ. For cells expressing multiple chromophores (YFP and CFP-tagged proteins), appropriate excitation lasers, laser intensities and emission filter bandwidths were selected to eliminate bleedthrough. For live-cell imaging, cells were kept out of the incubator for no more than 10 min. For fixed-cell imaging, H1299 cells were washed 3× with cold phosphate-buffered saline (PBS), then extracted for 60 s in cold CSK buffer, washed 3× with PBS, then fixed for 10 min in 2% PFA in PBS; XPV cells were washed 3× in cold PBS and then fixed for 15 min in methanol at −20°C. Post-fixation, all cells were covered with Vectashield Solution (Vector Laboratories) and imaged within 24 h. For foci quantification, five representative images containing ~60 cells were captured using 0.5 μm Z-stacks with a 40× using oil-immersion lens. After 3D projection, the number of cells clearly containing >100 nuclear foci were counted as a fraction of total chromophore-expressing cells.

Triton extraction, immunoprecipitation and immunoblotting

Extracts containing soluble and chromatin-associated proteins were prepared as previously described (30) by lysing cultured cells into cold cytoskeleton buffer (CSK buffer; 10 mM Pipes, pH 6.8, 100 mM NaCl, 300 mM sucrose, 3 mM $MgCl_2$, 1 mM EGTA, 1 mM DTT, 0.1 mM ATP, 1 mM Na_3VO_4, 10 mM NaF and 0.1% Triton X-100) supplemented with phosphatase and protease inhibitors (Roche Diagnostics, Indianapolis, IN, USA). For immunoprecipitation of whole cell lysate (WCL) or chromatin-bound proteins, Triton-insoluble proteins were released by sonication on ice for three 10-s intervals followed by centrifugation at 15 k *g* for 10 min. After normalizing to a protein concentration of 1 μg/μl, immunoprecipitation was conducted at 4°C by rotating overnight with HA-coupled or primary antibody-bound sepharose beads (Roche Diagnostics, Indianapolis, IN, USA). After immunoprecipitation, the beads were washed five times for 15 min in CSK buffer and then resuspended in minimum volume of Laemmli buffer. For immunoblot experiments, cell extracts or immunoprecipitates were separated by SDS-PAGE, followed by incubation overnight with the following primary antibodies: PCNA (sc-56), Chk1 (sc-7898), β-Actin (sc-130656), all from Santa Cruz Biotech (Santa Cruz, CA, USA); Polη (A301–231 A), Polκ (A301–975 A), Polι (A301–304 A) and R18 (A301–340 A), all from Bethyl Laboratories (Montgomery, TX, USA); and p53 (Ab-6) from Lab Vision (Fremont, CA, USA).

Genotoxin treatments

UV irradiation and benzo(a)pyrene diolepoxide (BPDE) treatment were performed as previously described (30), and BPDE (National Cancer Institute Carcinogen Repository) was dissolved in anhydrous Me_2SO and added directly to the growth medium as a 1000× stock to give various final concentrations, as indicated in the figure legends. For UVC treatment, the growth medium was removed from the cells, reserved and replaced with PBS. The plates were transferred to a UV cross-linker (Stratagene, Santa Clara, CA, USA) and then irradiated. The UVC dose delivered to the cells was confirmed with a UV radiometer (UVP BioImaging Systems, Upland, CA, USA). The reserved medium from the cells was replaced, and cells were returned to the incubator.

In vitro binding and ubiquitination assays

C-His_6-PCNA-expressing Top10 *Escherichia coli* (acquired from Marila Cordiero-Stone, UNC-CH) were collected and lysed in pH 8 buffer containing 50 mM $NaPO_4$, 300 mM NaCl, 20 mM imidazole and 0.1% Triton-X. After sonication and clarification, His_6-PCNA was purified over Ni-NTA beads. For His_6-PCNA pulldown experiments, HA-Rad18 was adenovirally expressed in H1299 cells alone or together with YFP-Polη and lysed in $NaPO_4$/NaCl/imidazole/Triton-X buffer. After sonication, clarification and normalization to a protein concentration of 1 μg/μl, cell lysates were rotated overnight at 4°C with His_6-PCNA on Ni-NTA beads. The beads were then washed five times in the same buffer before addition of Laemmli buffer, boiling and analysis by SDS-PAGE/Western Blot. For *in vitro* ubiquitination assays, H1299 cells expressing HA-Rad18 alone or together with YFP-Polη were lysed in $NaPO_4$/NaCl/imidazole/Triton-X buffer and immunoprecipitated with HA-sepharose beads. After washing the beads extensively, the beads were resuspended in 50 μl buffer and the following were added: His_6-PCNA (eluted from Ni-NTA beads with the same buffer plus 200 mM imidazole), 500 μM FLAG-ubiquitin, 10× Energy Regeneration Solution and 100 nM Ubiquitin Activating Enzyme (UBE1), all from Boston Biochem (Cambridge, MA, USA). After incubation for 16 h at 4°C, the mixture was mixed with Laemmli buffer, boiled and analysed by SDS-PAGE and Western Blot.

UV cytotoxicity assay

XPV or HDF cells were split into 24-well plates to a density of ~25%. Twelve hours later, the cells were infected with empty control adenovirus or adenovirus expressing YFP-Polη. Twenty-four hours after infection, the cells were exposed to UV light in the presence or absence of 1 mM caffeine. After 48 h, 50 mg/ml Thiazolyl Blue Tetrazolium Bromide (MTT) (Sigma-Aldrich, St. Louis, MO, USA) was added to each well and allowed to incubate at 37°C for 2 h. The cells were then rinsed with PBS and dissolved in 0.5 ml DMSO. The absorbance at 570 nm was then measured for each well and normalized to the sham-treated samples. The minimum dose of YFP-Polη that conferred resistance to UV light in XPV cells (~0.5×10^9 pfu/ml, Supplementary Figure S2) was determined by this method and used for survival assays.

Statistics

P values for statistical significance were determined by the unpaired Student's *t*-test with a two-tailed 95% confidence interval.

RESULTS

Polη promotes efficient Rad18-mediated PCNA monoubiquitination

Current models suggest that Rad18 plays proximal roles in TLS, chaperoning Polη to damaged chromatin and monoubiquitinating PCNA to stably engage Y family polymerases at sites of PRR (12,13). Unexpectedly, we observed deficient redistribution of Rad18 to nuclear foci (representing sites of replication stalling) in patient-derived XPV cells (XP115LO) following UV irradiation (Figure 1A and B, Supplementary Figure S1). In Polη-corrected XP115LO cells, Rad18 redistributed to nuclear foci in a UV-inducible manner and co-localized with Polη, indicating that Rad18 redistribution to repair foci is Polη dependent in XP115LO cells. Similar to results obtained with XPV cells, redistribution of Rad18 was defective in Polη-depleted H1299 cells (Figure 1C and E), which have intact TLS and rely on Polη for UV tolerance (30). As shown in Figure 1D, basal and UV-induced formation of Rad18 foci were dependent on Polη, indicating a general role for Polη in impacting Rad18 redistribution.

We next asked whether Polη status also affected PCNA-directed Rad18 E3 ligase activity. Polη-complemented XPV cells exhibited higher basal and damage-induced PCNA monoubiquitination compared with parental XPV cells, and Polη expression was associated with increased chromatin binding of Rad18 (Figure 1F). Conversely, UV-induced PCNA monoubiquitination was compromised in Polη-depleted normal human diploid fibroblasts (HDF) relative to Polη-replete controls (Figure 1G). Polη depletion thus partially phenocopies the expected effect of depleting RPA (Supplemental Figure S2), which is thought to initiate TLS by coating ssDNA and triggering ATR/Chk1 signalling and subsequent PCNA monoubiquitination (42,43). Rad18 redistribution and PCNA monoubiquitination were also attenuated in Polη-depleted cells after BPDE treatment (Supplementary Figure S3), indicating that the effect of Polη on Rad18 activity is not genotoxin specific.

Next, we determined whether increased Polη expression affects Rad18 and PCNA monoubiquitination. When expressed in HCT-116 cells at levels ranging from ~2- to 25-fold higher than endogenous, PCNA monoubiquitination increased in a dose-dependent fashion with Polη (Figure 1H). Importantly, PCNA monoubiquitination was not induced by Polη in isogenic Rad18-null HCT-116 cells, indicating that the effect of Polη on PCNA modification is Rad18 mediated (Figure 1H, right lane).

Potentially, the stimulatory effect of Polη expression on PCNA monoubiquitination could result (at least in part) from reduced PCNA de-ubiquitylation activity. Ubiquitin-Specific Protease 1 (USP1) is the only known PCNA-directed de-ubiquitylating (DUB) enzyme (44). To determine whether inhibition of USP1 activity contributes to Polη-dependent PCNA monoubiquitination, we determined the effects of Polη expression on PCNA modification in USP1-depleted cells. As expected, basal levels of PCNA monoubiquitination were increased by USP1 depletion (Figure 1H). However, Polη expression further increased PCNA monoubiquitination in cells lacking USP1 (compare lanes 2 and 8), both basally and 2 and 8 h after DNA damage. We conclude that that Polη stimulates PCNA monoubiquitination by Rad18 via USP1-independent mechanisms. We cannot exclude the formal possibility that Polη-dependent PCNA monoubiquitination is not mediated by reduced activity of putative alternative PCNA-directed DUBs. However, the results of Figure 1 and data presented below indicate that Polη facilitates redistribution of Rad18 to sites of DNA damage and promotes efficient PCNA monoubiquitination.

Rad18–Polη interaction is necessary for efficient PCNA monoubiquitination

Because Rad18 and Polη form a complex after DNA damage (31), we next asked whether Polη-dependent redistribution of Rad18 and PCNA monoubiquitination required Rad18–Polη interactions. The Polη-binding region of Rad18 has been mapped to amino acid (AA) residues 402–445 (Figure 2A) (31). Therefore, we determined the effect of Polη status on the activity of a Polη-interaction defective Rad18 mutant, Rad18-Δ(402–445), that retains E3 Ub-ligase activity and other DNA repair functions (31).

Consistent with *in vitro* binding studies (31), Rad18-Δ(402–445) failed to co-immunoprecipitate Polη from cell lysates (Figure 2B). To test how Polη–Rad18 binding affected subcellular Rad18 distribution, we depleted H1299 cultures of endogenous Rad18 and reconstituted with near-physiological levels of siRNA-resistant CFP-Rad18-WT or CFP-Rad18-Δ(402–445). As shown in Figure 2C and Supplementary Figure S4, co-expression of Polη significantly increased basal and damage-induced redistribution of Rad18-WT to nuclear foci but had no effect on the redistribution of Rad18-Δ(402–445). In replicate cultures of Rad18-complemented cells, Polη-induced PCNA monoubiquitination was severely compromised in cells complemented with Rad18-Δ(402–445) when compared with cells expressing Rad18-WT (Figure 2D, compare lanes 1 and 8 with 11 and 12). Therefore, Polη–Rad18 interactions are necessary for Polη-dependent PCNA monoubiquitination.

The stable engagement of TLS polymerases with stalled replication forks depends on their UBZ/UBM-mediated interactions with monoubiquitinated PCNA (12–14). As expected, the reduced PCNA monoubiquitination in cells complemented with Rad18-Δ(402–445) was associated with decreased Polη chromatin binding (Figure 2D) and reduced formation of Polη nuclear foci (Figure 2E and F), when compared with Rad18-WT-expressing cells. Thus, Rad18-Δ(402–445) partially recapitulates phenotypes conferred by the E3 ubiquitin ligase-deficient Rad18-C28F mutant (Figure 2A), including defective PCNA monoubiquitination (Figure 2G) and reduced recruitment of Polη to chromatin (Figure 2E and F).

Polη–PCNA interactions drive Rad18-mediated PCNA monoubiquitination

C-terminal Polη truncations are the most common defect in XPV (8,45,46), in which both the PIP box (47) and the

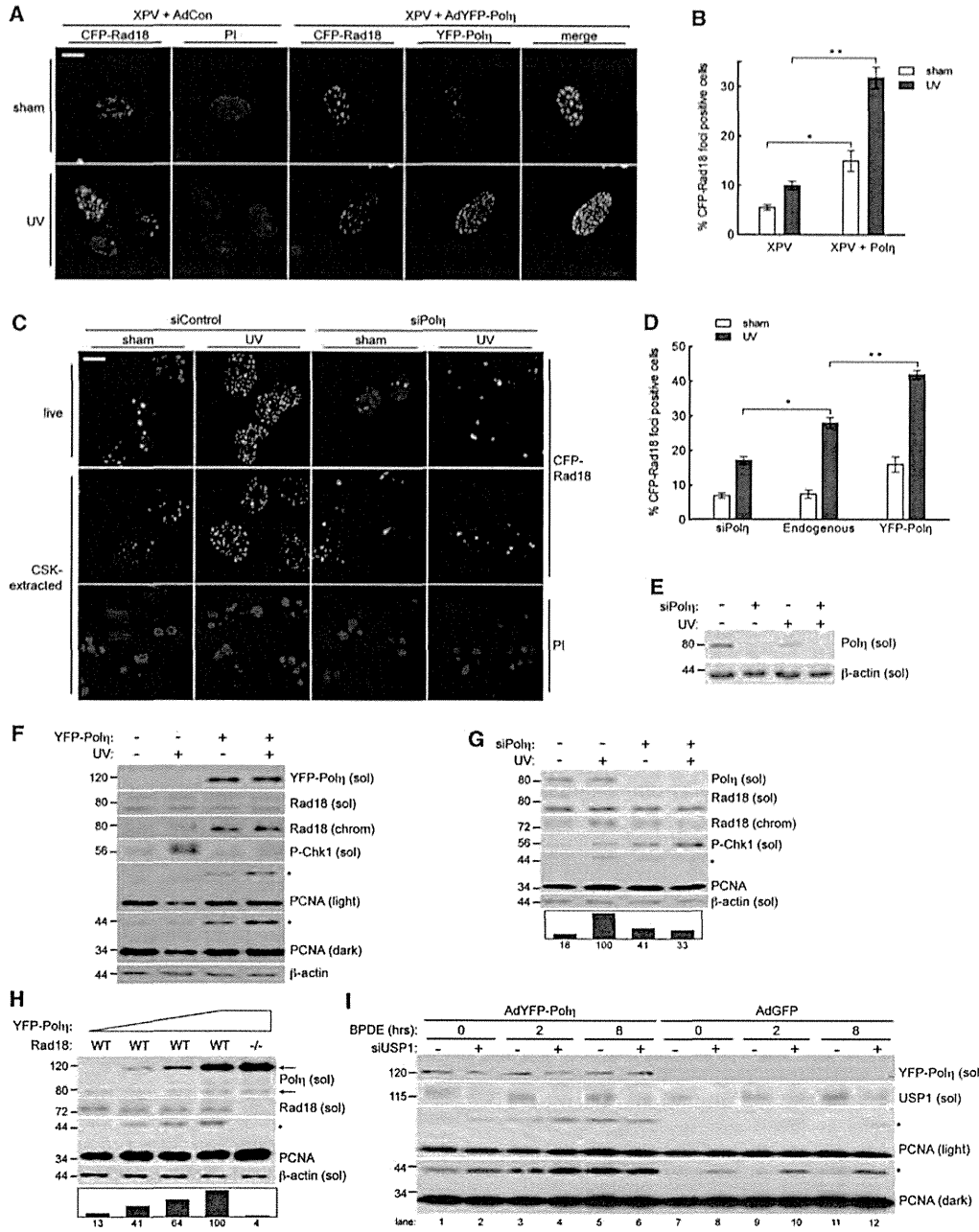

Figure 1. Polη promotes damage-induced Rad18 redistribution and PCNA monoubiquitination. (**A**) Representative images of CSK-extracted nuclei from CFP-Rad18-expressing XP115LO XPV cells co-infected with empty control adenovirus or adenovirus expressing YFP-Polη (at levels that restore UV tolerance—see Supplementary Figure S6) and exposed to UV ($10\,J/m^2$) or sham irradiated. Scalebar = 10 μm. (**B**) Quantification of CFP-Rad18 foci-positive H1299 nuclei as a percentage of CFP-Rad18-expressing cells as shown in (A); $*P = 0.0001$; $**P = 0.001$. Error bars = SEM. (**C**) Representative images of live (top) and CSK-extracted (bottom) nuclei from H1299 cells treated with non-targeting control siRNA (left) or siRNA targeting Polη (right) and imaged 2 h after sham or UV ($10\,J/m^2$) irradiation. Scalebar = 10 microns. (**D**) Quantification of CFP-Rad18 foci-positive nuclei as a percentage of CFP-Rad18-expressing cells as shown in (D). $*P = 0.001$; $**P = 0.0003$. (**E**) Immunoblot of fractionated lysates from H1299 cells expressing CFP-tagged Rad18 as shown in (D) and treated with non-targeting control siRNA or siRNA against Polη and then lysed 2 h after treatment with $10\,J/m^2$ UV or sham treated. (**F**) Immunoblot of fractionated lysates from XP115LO XPV cells treated with empty control adenovirus or adenovirus expressing YFP-Polη at levels shown in (A) and lysed 2 h after treatment with $10\,J/m^2$ UV. (**G**) Immunoblot of fractionated lysates from HDF cells treated with non-targeting control siRNA or siRNA against Polη and then lysed 2 h after treatment with $10\,J/m^2$ UV or sham irradiation. (**H**) Immunoblot of fractionated lysates from HCT-116 WT cells (lanes 1–4) or RAD18$^{-/-}$ cells (lane 5) treated with increasing titers of YFP-Polη adenovirus and lysed 24 h post-infection. Upper and lower arrows denote YFP-tagged and endogenous Polη, respectively. (**I**) Immunoblot of fractionated lysates from H1299 cells expressing empty control adenovirus or adenovirus expressing YFP-Polη and treated with non-targeting control siRNA or siRNA against USP1 and then lysed at indicated times after treatment with 200 nM BPDE. On all Western blots, asterisk denotes monoubiquitinated PCNA and bar graphs represent intensity of monoubiquitinated PCNA band relative to the maximum band on each film.

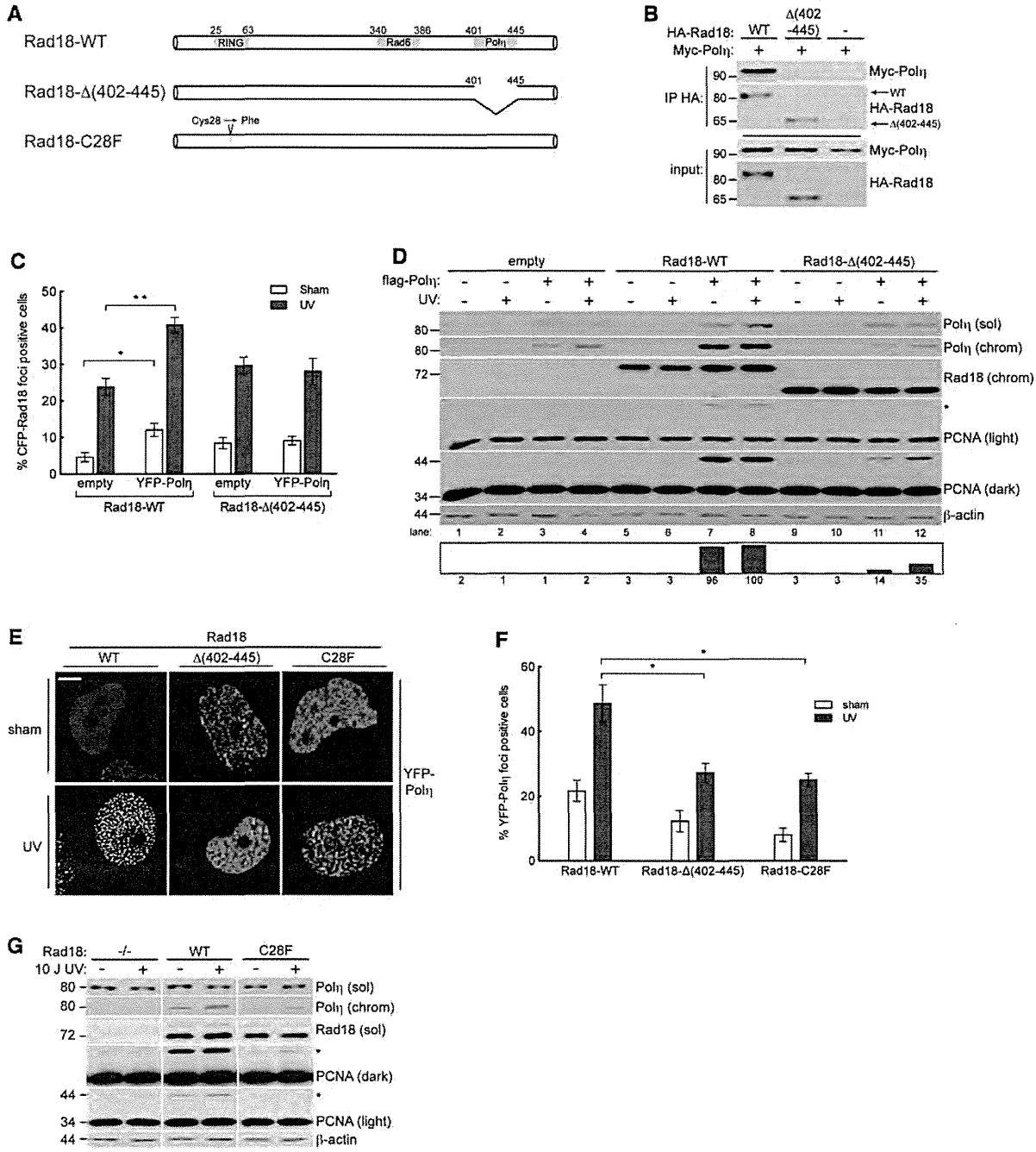

Figure 2. Physical interaction between Rad18 and Polη drives efficient damage-induced PCNA ubiquitination. (**A**) Schematic of Rad18-WT (top); Rad18-Δ(402–445), a Polη-binding deficient mutant lacking the Polη binding domain (AA 402–445); Rad18-C28F, an E3 ligase-inactive mutant in which the RING-finger cysteine has been substituted with phenylalanine. (**B**) Immunoblot analysis of anti-HA immunoprecipitates from H1299 cells co-expressing HA-Rad18-WT or HA-Rad18-Δ(402–445) with Myc-Polη. (**C**) Quantification of CFP-Rad18 foci-positive nuclei as a percentage of H1299 cells expressing CFP-Rad18-WT or CFP-Rad18-Δ(402–445) and treated with empty adenovirus or Myc-Polη-expressing adenovirus followed by UV (10 J/m^2) treatment or sham irradiation. *$P = 0.095$; **$P = 0.0006$. Error bars = SEM. (**D**) Immunoblots of fractionated lysates from Rad18-depleted H1299 cells that were reconstituted with siRNA-resistant Rad18-WT, Rad18-Δ(402–445), or empty vector (for control) alone or together with FLAG-Polη, followed by treatment with UV (10 J/m^2) or sham-irradiation. (**E**) Representative images of CSK-extracted nuclei from YPF-Polη expressing H1299 cells that were depleted of endogenous Rad18 and then reconstituted with siRNA-resistant Rad18-WT, or Rad18-Δ(402–445), or Rad18-C28F and treated with UV (10 J/m^2) or sham irradiated. Scalebar = 10 um. (**F**) Quantification of YFP-Polη foci-positive nuclei as a percentage of YFP-Polη-expressing cells in cultures complemented with Rad18-WT, Rad18-Δ(402–445), or Rad18-C28F as shown in (E). *upper $P = 0.026$, lower $P = 0.0238$. (**G**) Immunoblots of fractionated lysates from Rad18-depleted H1299 cells that were reconstituted with siRNA-resistant WT-Rad18, C28F-Rad18, or empty vector, and then treated with UV (10 J/m^2) or sham irradiated.

Rad18-binding domains (31) are deleted. To test whether Polη XPV C-terminal truncation mutants exhibit defects in Rad18 regulation, we complemented XPV cells with WT-Polη or similar levels of a common XPV Polη mutant that retains full catalytic activity (48) but fails to confer UV resistance [Polη-Δ(1–512), lacking residues 513–713, Figure 3A]. As expected, complementation of XPV cells with Polη-WT conferred normal Rad18 redistribution (Figure 3B and C) and resulted in increased PCNA monoubiquitination (Figure 3D). However, complementation of XPV cells with Polη-Δ(1–512) failed to restore Rad18 redistribution or PCNA monoubiquitination to the same extent as those complemented with Polη-WT (Figure 2B–D), indicating that the C-terminal domain of Polη is important not only for Polη chromatin binding, but also for Rad18 nuclear redistribution and Rad18-mediated PCNA monoubiquitination.

To test whether loss of PCNA binding contributes to defective PCNA monoubiquitination in Polη-Δ(1–512)-complemented XPV cells, we generated point mutations in the PIP box that abrogate PCNA binding (47) (Figure 3A). In Rad18-depleted cells complemented with physiological levels of Rad18-WT, Polη-WT, but not Polη-ΔPIP, promoted PCNA monoubiquitination by Rad18 (Figure 3E, compare lanes 7 and 8 with 11 and 12). Therefore, Polη–PCNA association via the PIP box of Polη contributes to maximal Rad18-mediated PCNA monoubiquitination.

Polη scaffolding mediates Rad18–PCNA association

Although Polη possesses a PIP box (47,49) and interacts directly with PCNA (47), no PCNA-interacting domain has been identified for Rad18, and the mechanism for association of Rad18 with PCNA is unknown. The Polη dependence of Rad18-mediated PCNA monoubiquitination (Figures 1–3) suggested that Polη may serve as a 'molecular bridge' or scaffold to facilitate Rad18–PCNA interactions. To test this hypothesis, we developed a cell-free system to determine the Polη dependence of PCNA–Rad18 interactions (if any). Recombinant PCNA was immobilized on Ni-NTA beads (or unloaded beads for controls) and incubated with extracts from cells expressing Rad18 alone or in combination with Polη. When extracts from Rad18-expressing cells were incubated with PCNA-Ni beads, we were unable to detect association between Rad18 and PCNA (Figure 3F, lane 1). However, we readily detected Rad18 association with immobilized PCNA incubated with lysates from Rad18 and Polη co-expressing cultures (Figure 3F, lane 2). Therefore, we conclude that Polη promotes Rad18–PCNA interactions or stabilizes Rad18–PCNA complexes.

We modified this cell-free assay to test whether the presence of Polη influenced PCNA monoubiquitination by Rad18. HA-Rad18 was expressed in UV-irradiated H1299 cells individually or in combination with Polη and then immunoprecipitated using anti-HA antibodies. The resulting immune complexes were then mixed with recombinant PCNA, E1, FLAG-ubiquitin and an ATP-regenerating system. As shown in Figure 3G, Rad18 immune complexes conjugated FLAG-ubiquitin to PCNA in a manner that was stimulated by Polη (compare lanes 2 and 3).

Taken together, the results of Figure 3 suggest that Polη promotes efficient PCNA monoubiquitination via a bridging mechanism that facilitates physical interaction between Rad18 and PCNA.

Polη-induced PCNA monoubiquitination is dissociable from catalytic activity

To test whether DNA polymerase activity was required for Polη to promote PCNA monoubiquitination, we generated a Polη mutant harbouring four inactivating point substitutions in conserved residues necessary for catalytic activity (40) (Figure 4A). Catalytically inactive mutant Polη (Polη-C.I.) and wild-type Polη both stimulated PCNA monoubiquitination to similar levels (Figure 4B). Additionally, Polη-C.I. caused Rad18 redistribution to nuclear foci in a manner nearly identical to Polη-WT (Figure 4C and D). Thus, the function of Polη in promoting Rad18-mediated PCNA monoubiquitination is dissociable from its catalytic role as a DNA polymerase.

To probe the molecular determinants of PCNA monoubiquitination induced by Polη, we performed structure–function studies using Polη truncation mutants that progressively eliminated AAs 1–400 spanning the catalytic domain (Figure 4A). Interestingly, when expressed at equal levels, the Polη-truncation mutants mobilized Rad18 to nuclear foci in a manner similar to Polη-WT (Figure 4E). A Polη truncation constituting only 300 C-terminal amino acids induced a level of PCNA monoubiquitination comparable with WT-Polη (Figure 4F). Therefore, the Rad18- and PCNA-binding C-terminus of Polη represents the minimal domain that is necessary and sufficient to regulate Rad18 activity and promote PCNA monoubiquitination.

Recent work identified a novel PIP box and UBZ-containing protein termed 'Spartan' that promotes PCNA monoubiquitination via a bridging mechanism between PCNA and Rad18, similar to that which we have defined for Polη (25). To compare the relative contribution of Spartan and Polη to Rad18-mediated PCNA monoubiquitination, we expressed FLAG-Polη or FLAG-Spartan in H1299 cells. When expressed at comparable levels, Polη induced an increase in PCNA monoubiquitination that was nearly 10-fold higher than that conferred by Spartan (Figure 4G) and siRNA-mediated knockdown of Polη decreased UV-induced PCNA monoubiquitination significantly more than Spartan knockdown (Supplementary Figure S5, compare lanes 4 and 6). Together, these data indicate that scaffolding of PCNA and Rad18 by Polη plays an important role in the regulation of PCNA monoubiquitination.

Y family polymerase specificity of Polη-dependent PCNA monoubiquitination

We next asked whether the stimulatory effect of Polη on Rad18 activity was shared by other Y-family TLS polymerases. Similar to Polη, Polκ associates with Rad18 (41), redistributes to form nuclear foci in response to DNA damage, and associates with PCNA via C-terminal PIP

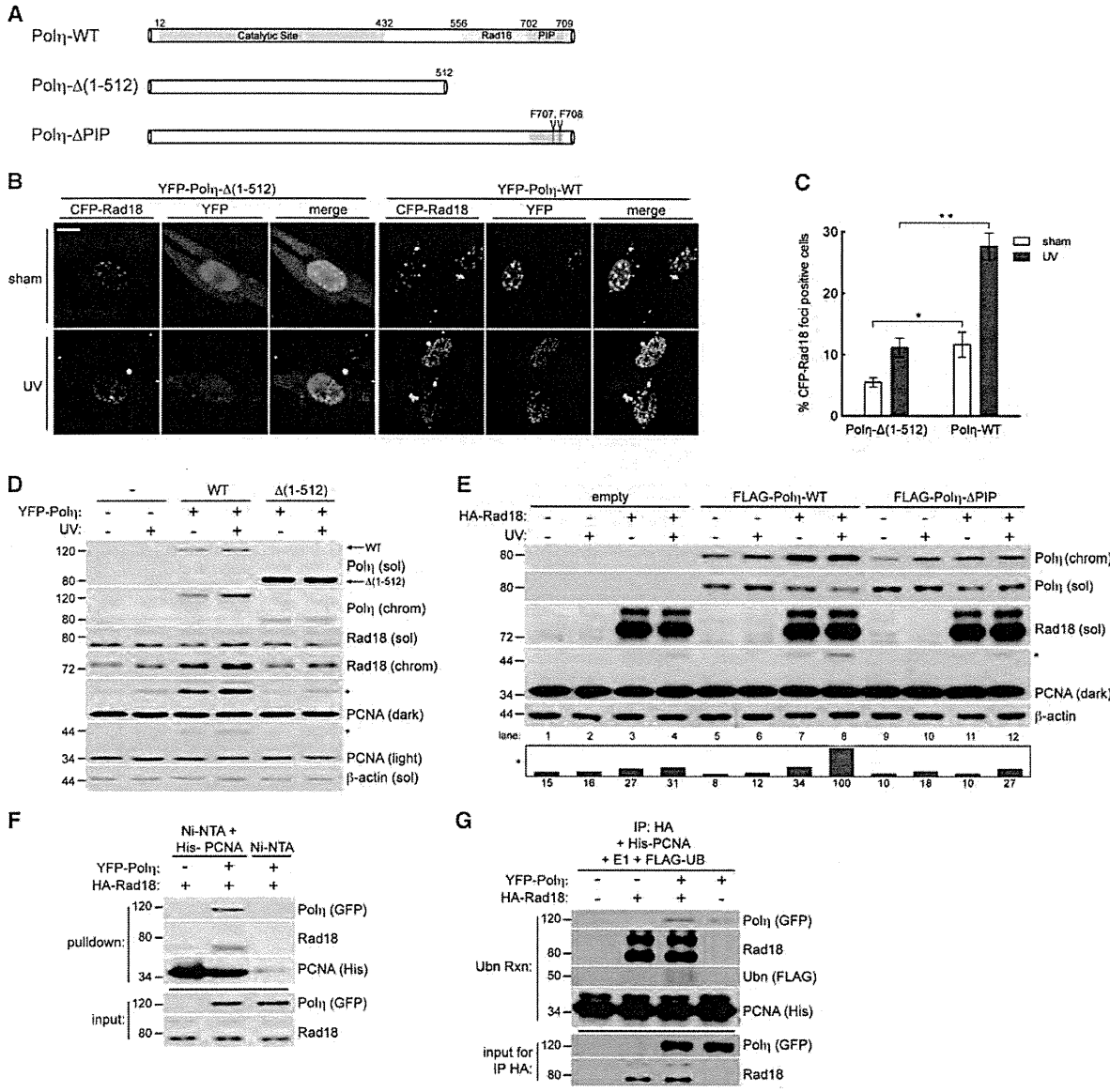

Figure 3. Polη physically bridges Rad18 and PCNA to promote efficient PCNA monoubiquitination after DNA damage. (**A**) Schematic of Polη-WT (top); Polη-Δ(1–512), a C-terminal truncation lacking AA 513–713 (middle); and Polη-ΔPIP, full length Polη with two PIP box phenylalanines mutated to alanine (bottom). (**B**) Representative images of CSK-extracted nuclei from XPV cells that were co-infected with CFP-Rad18 and YFP-Polη-Δ(1–512) adenovirus (left) or YFP-Polη-WT (right) and treated with UV (10 J/m^2) or sham irradiated. Scalebar = 10 um. (**C**) Quantification of CFP-Rad18 foci-positive nuclei as a percentage of CFP-Rad18-expressing XPV cells expressing YFP-Polη-Δ(1–512) or YFP-Polη-WT adenovirus. *upper $P = 0.018$; **$P = 0.0001$; Error bars = SEM. (**D**) Immunoblots of fractionated lysates from XPV cells complemented with Polη-WT or Polη-Δ(1–512) and treated with 10 J/m^2 UV. (**E**) Immunoblots of fractionated lysates from Rad18-depleted H1299 cells that were reconstituted with siRNA-resistant Rad18-WT together with FLAG-tagged Polη-WT or Polη-ΔPIP and treated with sham or 10 J/m^2 UV. (**F**) *In vitro* pulldown assay. His$_6$-PCNA-loaded Nickel beads (or unloaded beads) were incubated with lysates from UV-irradiated H1299 cells expressing HA-Rad18 or both HA-Rad18 and YFP-Polη. (**G**) *In vitro* ubiquitination assay. HA-Rad18 complexes immunoprecipitated from UV-irradiated H1299 cells expressing HA-Rad18 alone or in combination with YFP-Polη were mixed with recombinant His$_6$-PCNA, E1, FLAG-ubiquitin, and an ATP-regenerating system and conjugated FLAG-Ub was detected by immunoblotting with anti-FLAG antibodies.

box. Therefore, for the purpose of comparison with Polη, we determined the effects of manipulating Polκ expression levels on PCNA monoubiquitination. In contrast with Polη knockdown, Polκ depletion did not attenuate PCNA monoubiquitination basally or after genotoxin treatment (Figure 5A). Even when expressed at levels ~15-fold higher than Polη, Polκ did not induce the robust PCNA monoubiquitination response elicited by Polη (Figure 5B). Polκ also induced far less Rad18 redistribution to chromatin. Hence, the role of Polη in promoting genotoxin-induced PCNA monoubiquitination is not shared by all Y-family TLS polymerases.

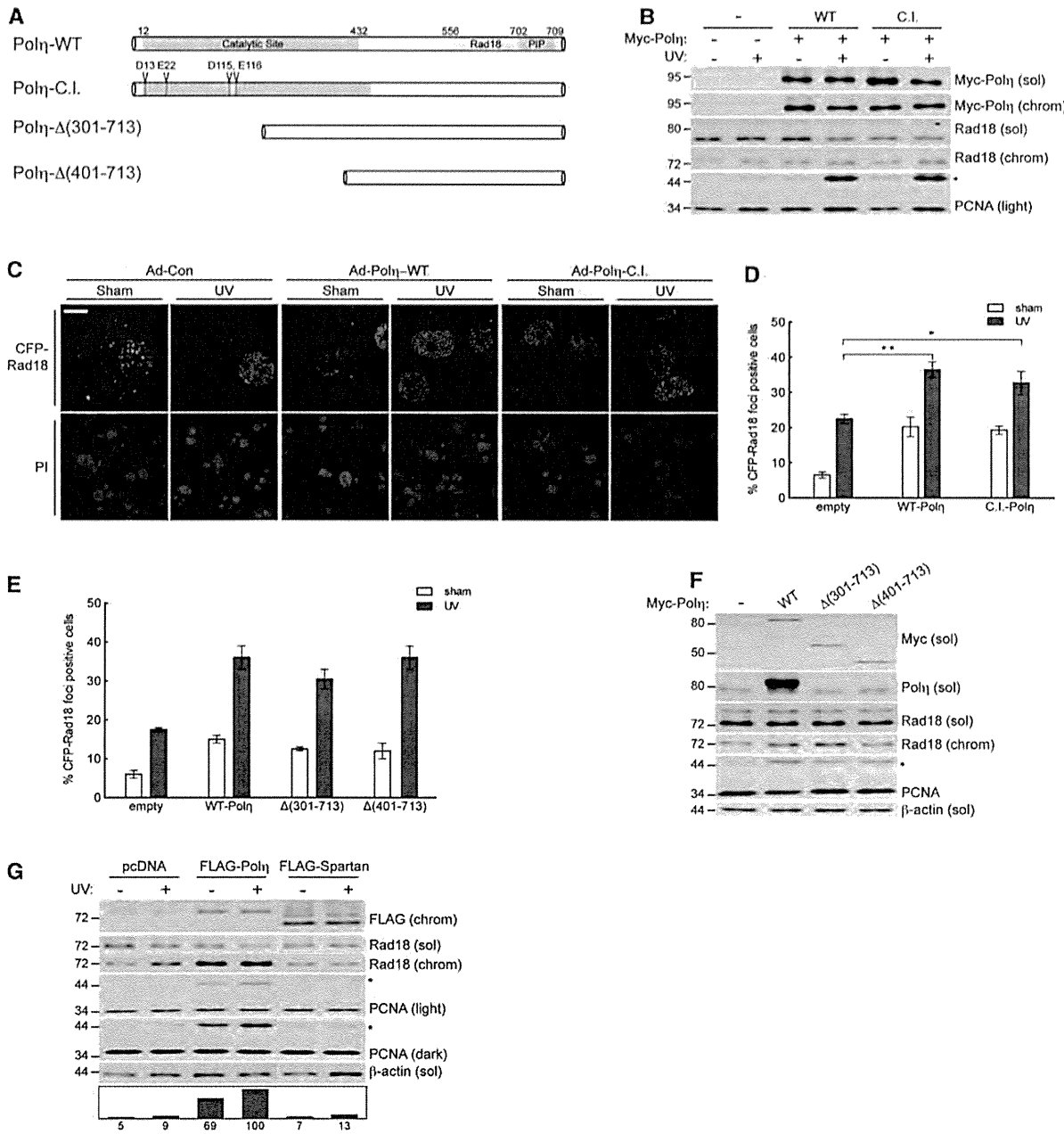

Figure 4. Physical bridging of Rad18 and PCNA by Polη is dissociable from its DNA polymerase activity. (**A**) Schematic of Polη-WT (top); full-length catalytically inactive Polη, Polη-C.I, in which amino acids D13, E22, D115 and E116 are mutated to alanine; and N-terminal Polη truncation mutants, Polη-Δ(301–713) and Polη-Δ(401–713). (**B**) Immunoblots of fractionated lysates from Myc-Polη-WT or Myc-Polη-C.I.-expressing H1299 cells that were treated with UV ($10\,J/m^2$) or sham irradiated. (**C**) Representative images of CSK-extracted nuclei from H1299 cells that were co-infected with CFP-Rad18 and empty control adenovirus (left), Myc-Polη-WT (middle) or Myc-Polη-C.I. (right) and treated with UV ($10\,J/m^2$) or sham irradiated. Scalebar = 10 um. (**D**) Quantification of CFP-Rad18 foci-positive nuclei as a percentage of CFP-Rad18-expressing H1299 cells expressing empty control adenovirus, Myc-Polη-WT or Myc-Polη-C.I. $^{**}P = 0.0016$; $^{*}P = 0.0287$; Error bars = SEM. (**E**) Quantification of CFP-Rad18 foci-positive nuclei as a percentage of CFP-Rad18-expressing H1299 cells expressing empty control adenovirus, Myc-Polη-WT, Myc-Polη-Δ(301–713) or Myc-Polη-Δ(401–713). Error bars = SEM. (**F**) Immunoblot of fractionated lysates from H1299 cells expressing empty control adenovirus, Myc-Polη-WT, Myc-Polη-Δ(301–713) or Myc-Polη-Δ(401–713). (**G**) Immunoblot of fractionated lysates from H1299 cells expressing empty vector control, FLAG-Polη or FLAG-Spartan and lysed 2 h after treatment with $10\,J/m^2$ UV or sham treatment.

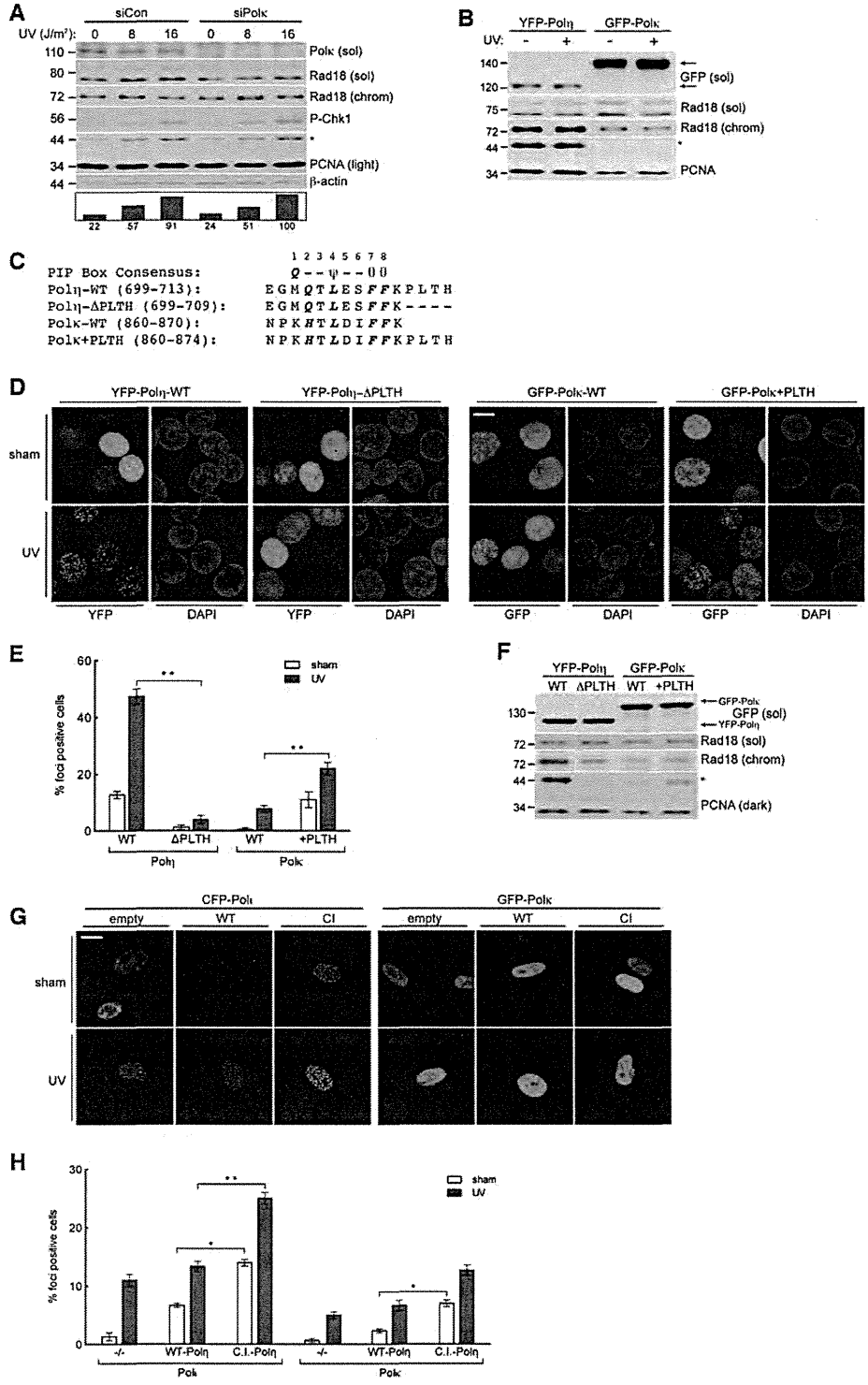

Figure 5. High-affinity interaction with PCNA drives Polη-specific induction of PCNA monoubiquitination. (**A**) Immunoblot of fractionated lysates from control or Polκ-depleted H1299 cells that were lysed 2 h after treatment with UV (10 J/m2) or sham irradiation. (**B**) Immunoblot of fractionated lysates from H1299 cells expressing YFP-Polη or GFP-Polκ and lysed 2 h after treatment with UV (10 J/m^2) or sham irradiated. (**C**) Sequence of the C-terminus of Polη and Polκ and the mutants used in domain-swap experiments: Polη-ΔPLTH and Polκ+PLTH. PIP-box consensus amino acids are in bold, where ψ = I/L/M; θ = Y/F. (**D**) Representative images of CSK-extracted nuclei from H1299 cells that were infected with GFP-Polκ-WT, GFP-Polκ+PLTH, YFP-Polη-WT or YFP-Polη-ΔPLTH and treated with 10 J/m^2 UV or sham irradiated. Scalebar = 10 μm. (**E**) Quantification of foci-positive nuclei as a percentage of H1299 cells expressing in YFP-Polη-WT, YFP-Polη-ΔPLTH, GFP-Polκ-WT or GFP-Polκ+PLTH.

(continued)

Because Polη and Polκ both associate with Rad18 after DNA damage (30,41), differences in Rad18 binding do not explain the inability of Polκ to promote PCNA monoubiquitination. We therefore hypothesized that differences in TLS polymerase–PCNA binding account for the differential contributions of Polη and Polκ to PCNA monoubiquitination. Domains flanking the PIP boxes in the various Y family members confer dramatically different PCNA-binding affinities (49); specifically, the high PCNA-binding affinity of Polη relative to other TLS polymerases is attributed in large part to the 'PLTH' sequence immediately C-terminal to its PIP box (Figure 5C).

To test whether PCNA-binding affinity influences relative PCNA monoubiquitination activity, we performed domain-swap experiments in which we removed the PLTH motif from Polη (generating Polη-ΔPLTH) or added it to Polκ (generating Polκ+PLTH) (Figure 5C). We then compared the subcellular distribution of wild-type and mutant forms of Polη and Polκ. As expected, Polη-ΔPLTH showed reduced nuclear focus formation and was also compromised for PCNA monoubiquitination activity relative to Polη-WT (Figure 5D and F). Conversely, whereas Polκ-WT was localized diffusely throughout the nucleus, Polκ+PLTH showed a focal distribution pattern more similar to that of Polη-WT. Interestingly, Polκ+PLTH induced more robust PCNA monoubiquitination than Polκ-WT (Figure 5F), demonstrating that addition of the PLTH (from the Polη PIP) to the Polκ PIP increases its ability to induce PCNA monoubiquitination. Therefore, high affinity binding of Polη to PCNA confers the unique ability among Y-family polymerases to promote PCNA monoubiquitination.

DNA damage-induced PCNA monoubiquitination contributes to the PCNA binding of all Y-family TLS polymerases (11–13). We hypothesized that Polη would influence other Y-family TLS polymerases by facilitating PCNA monoubiquitination, independently of its catalytic activity. Therefore, we compared the UV-inducible redistribution of Polι and Polκ in parental XPV cells or XPV cells reconstituted with Polη-WT or Polη-C.I. Consistent with prior studies (50,51), we found that basal and UV-induced Polι and Polκ redistribution to nuclear foci was higher in Polη-WT-reconstituted XPV cells compared with the Polη-defective parental cell line (Figure 5G and H). Importantly, we found that Polη-C.I. dramatically increased both basal and UV-induced redistribution of Polι and Polκ to nuclear foci. We conclude that cells expressing full-length catalytically inactive Polη retain Rad18-stimulatory activity, which in turn promotes recruitment of alternative error-prone polymerases to stalled replication forks.

p53 promotes PCNA monoubiquitination via transcriptional induction of Polη

Because Rad18-mediated PCNA monoubiquitination was sensitive to Polη expression, it was of interest to determine relative levels of Rad18 and Polη within cells. Therefore, we expressed an in-frame fusion of full-length Polη and full-length Rad18 in cultured cells, which allowed us to perform quantitative comparison of each endogenous protein relative to the Rad18–Polη fusion (Figure 6A) using appropriate antibodies.

At expression levels comparable with endogenous Polη, the Rad18–Polη fusion protein was nearly undetectable in immunoblots with anti-Rad18 antibody (Rad18 light), and prolonged exposures revealed that expression of the fusion at these levels was substantially lower than endogenous Rad18 (Rad18 dark). This surprising result demonstrated that cellular Rad18 protein expression is several orders of magnitude higher than Polη in human cells; we estimate that Rad18 expression exceeds Polη by ~75-fold. Importantly, expression of the Rad18–Polη fusion protein to a level double that of endogenous Polη (and negligible compared with endogenous Rad18) induced a 6-fold increase in PCNA monoubiquitination (right lane), showing that Rad18-mediated PCNA monoubiquitination is highly sensitive to Polη levels. These findings prompted us to determine whether physiologically relevant changes in Polη expression influence PCNA monoubiquitination.

POLH is a transcriptional target of activated p53, and DNA damage stimulates p53-dependent increases in Polη protein expression (52). Because endogenous Polη levels are limiting for Rad18 activity, we hypothesized that p53-induced Polη expression contributes to PCNA monoubiquitination. Therefore, we compared UV-induced PCNA monoubiquitination in WT HCT-116 cells and an isogenic p53-null HCT-116 line (Figure 6B). As expected, Polη protein levels were lower in p53-null cells (compared with WT) after UV. Interestingly, PCNA was monoubiquitinated after UV treatment in a manner that was temporally co-incident with Polη expression in p53-expressing HCT-116 cells, but not in $p53^{-/-}$ cells.

To test whether the p53-induced PCNA monoubiquitination was Polη dependent, we depleted Polη in p53-null H1299 cells that were transfected with empty vector or pcDNAp53. As shown in Figure 6C, transient expression of p53 led to concomitant increases in Polη expression and UV-induced PCNA monoubiquitination (compare lanes 1 and 2 with 5 and 6). Importantly, Polη depletion severely impaired PCNA monoubiquitination in p53-expressing cells compared to controls. Therefore, the

Figure 5. Continued
*left $P = 0.0001$; **$P = 0.0004$; Error bars = SEM. (**F**) Immunoblot of fractionated lysates from H1299 expressing YFP-Polη-WT, YFP-Polη-ΔPLTH, GFP-Polκ-WT or GFP-Polκ+PLTH. (**G**) Representative images of CSK-extracted nuclei from XPV cells that were co-infected with CFP-Polι or GFP-Polκ and empty control adenovirus (left), Myc-Polη-WT (middle) or Myc-Polη-C.I. and treated with UV (10 J/m^2) or sham irradiated. Scalebar = 10 μm. (**H**) Quantification of CFP-Polι foci-positive nuclei as a percentage of CFP-Polι-expressing XPV cells (left) and GFP-Polκ foci-positive nuclei as a percentage of GFP-Polκ-expressing XPV cells (right), after co-infection with empty control adenovirus, Myc-Polη-WT or Myc-Polη-C.I. and treatment with UV (10 J/m^2) or sham irradiation. *left $P = 0.0009$; **$P = 0.0004$, *right $P = 0.0022$; Error bars = SEM.

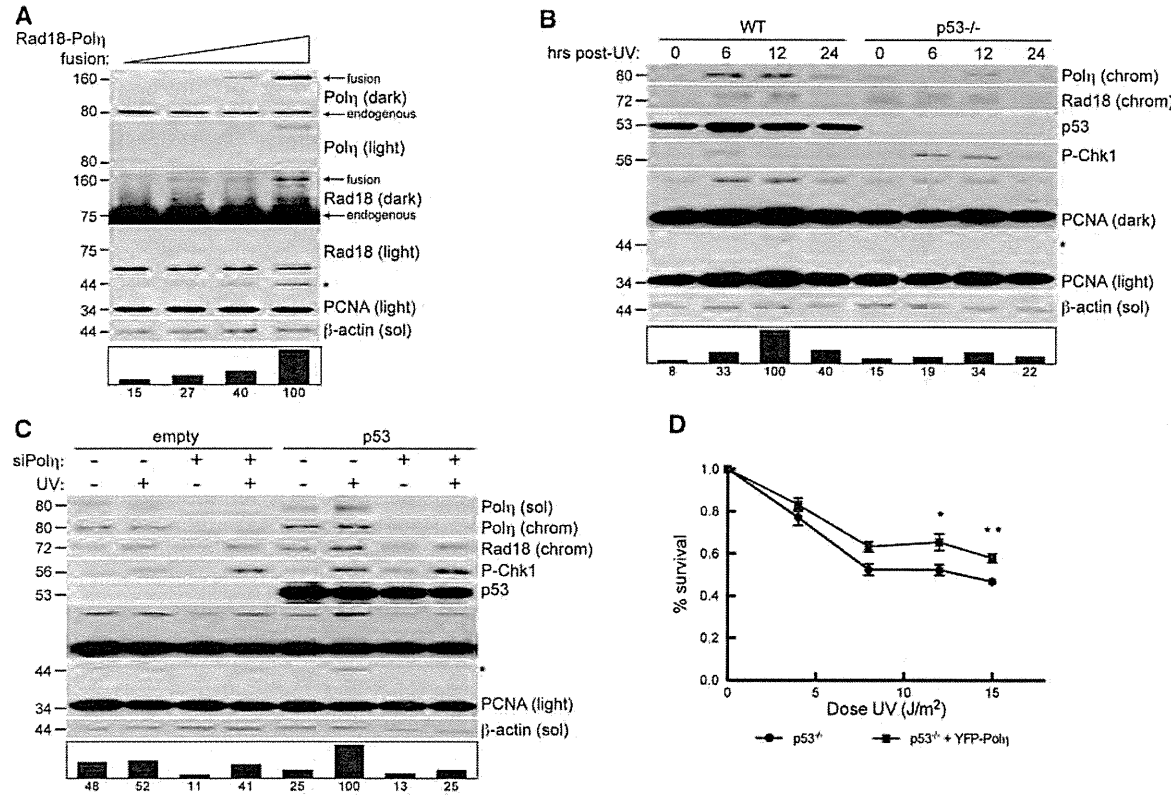

Figure 6. Rad18–Polη interaction is checkpoint sensitive and p53 regulated in response to DNA damage. (**A**) Immunoblots of fractionated lysates from H1299 cells transfected with increasing quantities of pACCMV-Rad18-Polη fusion construct. (**B**) Immunoblot of fractionated lysates from HCT-116 WT or HCT-116 $p53^{-/-}$ cells that were UV treated (30 J/m^2) and lysed at indicated times after irradiation. (**C**) Immunoblots of fractionated lysates of H1299 cells that were transfected with empty pcDNA as control or pcDNA-p53, followed by non-targeting control siRNA or siRNA against Polη. Cells were lysed 6 h after 10 J/m^2 UV. (**D**) UV sensitivity of WT or $p53^{-/-}$ HDF incubated in 1 mM caffeine and exposed to increasing doses of UV. Cells were infected with YFP-Polη adenovirus at a dose that confers UV survival in XP115LO cells (see Supplementary Figure S6). $^{**}P = 0.0305$ at 12 J/m^2. $^{**}P = 0.0036$ at 15 J/m^2.

p53-dependent component of PCNA monoubiquitination is Polη-mediated.

Because loss of p53 sensitizes normal fibroblasts, but not XPV cells, to UV (53,54), we hypothesized that the UV protection conferred by Polη is mediated by p53. To test this hypothesis, we compared UV survival in p53-depleted HDF cells infected with 'empty' control adenovirus or adenovirus expressing Polη at levels that confer UV survival in XPV fibroblasts (Supplementary Figure S6). We found that Polη expression modestly, but significantly, increased UV survival in $p53^{-/-}$ cells (Figure 6D). Therefore, loss of p53-mediated Polη regulation indeed contributed to the UV sensitivity of p53 null fibroblasts. Together, these results suggest that Polη facilitates PCNA monoubiquitination in a p53-dependent manner, thereby revealing a novel link between the p53 pathway and TLS (Figure 7).

DISCUSSION

The results described here are consistent with existing models of TLS pathway activation involving an initial redistribution of the Rad18–Polη complex to the vicinity of damaged DNA (most likely via association of Rad18 with RPA-coated ssDNA) (23,55). However, our results extend current models in that we propose Rad18 is in turn targeted to PCNA, its relevant substrate at the stalled replication fork, by Polη (Figure 7). Specifically, the extreme C-terminus of Polη physically bridges Rad18 and PCNA to stimulate PCNA monoubiquitination (Figure 3), a function unique to Polη among TLS polymerases and fully dissociable from its TLS polymerase activity. The results of this study challenge the notion that TLS constitutes a simple linear pathway in which Rad18 acts upstream of Polη to promote TLS. Instead, we propose that Rad18 and Polη play mutually dependent roles in TLS pathway activation.

Non-catalytic effector functions have been identified for other participants of the DDR, including Rev1 (56), Rad18 (31), NBS1 (57) and Chk1 (58), but this is the first demonstration of a DNA polymerase-independent activity for Polη. A non-catalytic role for Polη in stimulating PCNA monoubiquitination helps explain results of recent studies by other labs. For example, XPV cells are hypersensitive to BPDE and other genotoxins whose DNA lesions are not bypassed by

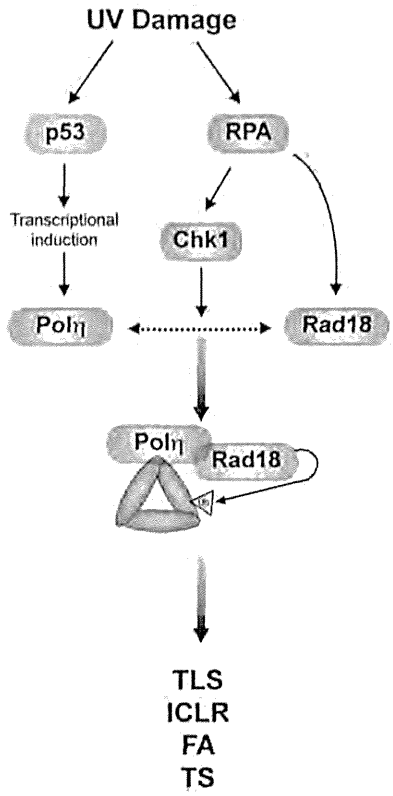

Figure 7. Contributions of p53 and Chk1 signalling to Polη-facilitated PCNA monoubiquitination. UV-induced p53 activity leads to transcriptional induction of Polη expression (left). RPA-coated ssDNA generated through helicase-polymerase uncoupling directly recruits Rad18 and promotes Polη-Rad18 association via Chk1 signalling (right), thereby stimulating PCNA monoubiquitination and dependent DDR pathways.

Polη (33,34); clearly, a polymerase-independent function of Polη that promotes PCNA monoubiquitination and activation of Polκ (the TLS polymerase that mediates bypass of BPDE adducts) explains the BPDE sensitivity of XPV cells. In other studies, catalytically dead Polη mutants conferred DNA damage tolerance (36,59) and mutagenesis (35,36). Because PCNA monoubiquitination at K164 is necessary for tolerance of UV and other genotoxins (15–17), restoration of UV survival by catalytically dead Polη (36) is explained by its scaffold function that promotes PCNA monoubiquitination, thus recruiting other TLS polymerases that facilitate tolerance, albeit at a cost of increased mutagenesis.

The Polη scaffolding function identified here has important implications for the molecular basis of genetic instability in XPV patients. Mutagenesis in XPV cells is widely believed to result solely from deficient Polη polymerase activity (60), leading to error-prone TLS of UV-damaged DNA by alternative and inappropriate TLS polymerases (10). Many XPV mutations encode C-terminally-truncated forms of Polη that lack Rad18- and PCNA-binding domains (45). However, in XPV cells in which Polη catalytic activity is perturbed while Rad18-PCNA bridging activity remains intact, high rates of UV-induced mutation frequencies may be conferred not only by loss of thymine dimer bypass activity by Polη, but also by stimulation of Rad18-mediated PCNA monoubiquitination and recruitment of alternative error-prone DNA polymerases.

Our finding that cellular Rad18 expression vastly exceeds Polη was unexpected, yet fully explains why PCNA monoubiquitination is exquisitely sensitive to slight alterations in Polη levels (Figure 6). Potentially, any process that affects Polη expression (52), stability (61–63), or nuclear localization (64) or its association with Rad18 is likely to affect PCNA monoubiquitination and in turn influence TLS. Indeed, we show here that transcriptional induction of *POLH* by p53 contributes to PCNA monoubiquitination. The Polη-Rad18 interaction is dependent on checkpoint signalling via Chk1 (30). Therefore, the results of this study may explain the long-standing observation that Chk1 signalling is required for efficient PCNA monoubiquitination (41,58). In fact, the Rad18-Δ(402–445) mutant in this study that failed to monoubiquitinate PCNA inducibly in response to Polη expression lacks the Chk1-dependent phosphorylation sites required for Polη binding (30). Therefore, the Polη-dependent mechanism for PCNA monoubiquitination described here may provide the basis for cross-talk between TLS and multiple processes including p53 signalling and the S-phase checkpoint.

Several DNA damage-tolerance pathways depend on PCNA monoubiquitination, including replication fork restart (20), template switching (19), intrastrand cross-link repair (21) and the Fanconi Anaemia pathway (22). Hence, Polη contributes to cross-talk between multiple DDR pathways via PCNA monoubiquitination; loss of this element of the DDR in XPV underscores the importance of their orchestrated convergence to preserve genetic stability.

SUPPLEMENTARY DATA

Supplementary Data are available at NAR Online: Supplementary Figures 1–6.

ACKNOWLEDGEMENTS

We are grateful to Dr. Hauro Ohmori, Dr. Yuichi Machida and Dr. James Wohlschlegel for helpful discussions. We thank Dr. Marila Cordiero Stone (UNC-CH, USA) for the C-His_6-PCNA bacterial expression plasmid and XP115LO (XPV) cells. We thank Dr. Bill Kaufmann (UNC-CH, USA) for the WT and p53-depleted HDF. We thank Dr. Lee Zou and Dr. Richard Centore (MGH, USA) for providing Spartan constructs. We are grateful to Dr. Bronwyn M. Gunn for critical reading of the manuscript.

FUNDING

National Institutes of Health (NIH) [E509558 and E5016280 to C.V. and 1F30ES019449 to M.D.]. Funding for open access charge: NIH [E509558, E5016280].

Conflict of interest statement. None declared.

REFERENCES

1. Friedberg,E.C. (2003) DNA damage and repair. *Nature*, **421**, 436–440.
2. Friedberg,E.C., Wagner,R. and Radman,M. (2002) Specialized DNA polymerases, cellular survival, and the genesis of mutations. *Science*, **296**, 1627–1630.
3. Friedberg,E.C., Fischhaber,P.L. and Kisker,C. (2001) Error-prone DNA polymerases: novel structures and the benefits of infidelity. *Cell*, **107**, 9–12.
4. Goodman,M.F. (2002) Error-prone repair DNA polymerases in prokaryotes and eukaryotes. *Annu. Rev. Biochem.*, **71**, 17–50.
5. Ohmori,H., Friedberg,E.C., Fuchs,R.P., Goodman,M.F., Hanaoka,F., Hinkle,D., Kunkel,T.A., Lawrence,C.W., Livneh,Z., Nohmi,T. *et al.* (2001) The Y-family of DNA polymerases. *Mol. Cell*, **8**, 7–8.
6. Johnson,R.E., Prakash,S. and Prakash,L. (1999) Efficient bypass of a thymine-thymine dimer by yeast DNA polymerase, Poleta. *Science*, **283**, 1001–1004.
7. Lehmann,A.R., Kirk-Bell,S., Arlett,C.F., Paterson,M.C., Lohman,P.H., de Weerd-Kastelein,E.A. and Bootsma,D. (1975) Xeroderma pigmentosum cells with normal levels of excision repair have a defect in DNA synthesis after UV-irradiation. *Proc. Natl Acad. Sci. USA*, **72**, 219–223.
8. Masutani,C., Kusumoto,R., Yamada,A., Dohmae,N., Yokoi,M., Yuasa,M., Araki,M., Iwai,S., Takio,K. and Hanaoka,F. (1999) The XPV (xeroderma pigmentosum variant) gene encodes human DNA polymerase eta. *Nature*, **399**, 700–704.
9. Ohashi,E., Ogi,T., Kusumoto,R., Iwai,S., Masutani,C., Hanaoka,F. and Ohmori,H. (2000) Error-prone bypass of certain DNA lesions by the human DNA polymerase kappa. *Genes Dev.*, **14**, 1589–1594.
10. Wang,Y., Woodgate,R., McManus,T.P., Mead,S., McCormick,J.J. and Maher,V.M. (2007) Evidence that in xeroderma pigmentosum variant cells, which lack DNA polymerase eta, DNA polymerase iota causes the very high frequency and unique spectrum of UV-induced mutations. *Cancer Res.*, **67**, 3018–3026.
11. Freudenthal,B.D., Gakhar,L., Ramaswamy,S. and Washington,M.T. (2010) Structure of monoubiquitinated PCNA and implications for translesion synthesis and DNA polymerase exchange. *Nat. Struct. Mol. Biol.*, **17**, 479–484.
12. Kannouche,P.L., Wing,J. and Lehmann,A.R. (2004) Interaction of human DNA polymerase eta with monoubiquitinated PCNA: a possible mechanism for the polymerase switch in response to DNA damage. *Mol. Cell*, **14**, 491–500.
13. Bienko,M., Green,C.M., Crosetto,N., Rudolf,F., Zapart,G., Coull,B., Kannouche,P., Wider,G., Peter,M., Lehmann,A.R. *et al.* (2005) Ubiquitin-binding domains in Y-family polymerases regulate translesion synthesis. *Science*, **310**, 1821–1824.
14. Plosky,B.S., Vidal,A.E., Fernandez de Henestrosa,A.R., McLenigan,M.P., McDonald,J.P., Mead,S. and Woodgate,R. (2006) Controlling the subcellular localization of DNA polymerases iota and eta via interactions with ubiquitin. *EMBO J.*, **25**, 2847–2855.
15. Brown,S., Niimi,A. and Lehmann,A.R. (2009) Ubiquitination and deubiquitination of PCNA in response to stalling of the replication fork. *Cell Cycle*, **8**, 689–692.
16. Hendel,A., Krijger,P.H., Diamant,N., Goren,Z., Langerak,P., Kim,J., Reissner,T., Lee,K.Y., Geacintov,N.E., Carell,T. *et al.* (2011) PCNA ubiquitination is important, but not essential for translesion DNA synthesis in mammalian cells. *PLoS Genet.*, **7**, e1002262.
17. Krijger,P.H., van den Berk,P.C., Wit,N., Langerak,P., Jansen,J.G., Reynaud,C.A., de Wind,N. and Jacobs,H. (2011) PCNA ubiquitination-independent activation of polymerase eta during somatic hypermutation and DNA damage tolerance. *DNA Repair (Amst)*, **10**, 1051–1059.
18. Niimi,A., Brown,S., Sabbioneda,S., Kannouche,P.L., Scott,A., Yasui,A., Green,C.M. and Lehmann,A.R. (2008) Regulation of proliferating cell nuclear antigen ubiquitination in mammalian cells. *Proc. Natl Acad. Sci. USA*, **105**, 16125–16130.
19. Lin,J.R., Zeman,M.K., Chen,J.Y., Yee,M.C. and Cimprich,K.A. (2011) SHPRH and HLTF act in a damage-specific manner to coordinate different forms of postreplication repair and prevent mutagenesis. *Mol. Cell*, **42**, 237–249.
20. Ciccia,A., Nimonkar,A.V., Hu,Y., Hajdu,I., Achar,Y.J., Izhar,L., Petit,S.A., Adamson,B., Yoon,J.C., Kowalczykowski,S.C. *et al.* (2012) Polyubiquitinated PCNA recruits the ZRANB3 translocase to maintain genomic integrity after replication stress. *Mol. Cell*, **47**, 396–409.
21. Yang,K., Moldovan,G.L. and D'Andrea,A.D. (2010) RAD18-dependent recruitment of SNM1A to DNA repair complexes by a ubiquitin-binding zinc finger. *J. Biol. Chem.*, **285**, 19085–19091.
22. Geng,L., Huntoon,C.J. and Karnitz,L.M. (2010) RAD18-mediated ubiquitination of PCNA activates the Fanconi anemia DNA repair network. *J. Cell Biol.*, **191**, 249–257.
23. Davies,A.A., Huttner,D., Daigaku,Y., Chen,S. and Ulrich,H.D. (2008) Activation of ubiquitin-dependent DNA damage bypass is mediated by replication protein a. *Mol. Cell*, **29**, 625–636.
24. Huttner,D. and Ulrich,H.D. (2008) Cooperation of replication protein A with the ubiquitin ligase Rad18 in DNA damage bypass. *Cell Cycle*, **7**, 3629–3633.
25. Centore,R.C., Yazinski,S.A., Tse,A. and Zou,L. (2012) Spartan/C1orf124, a reader of PCNA ubiquitylation and a regulator of UV-induced DNA damage response. *Mol. Cell*, **46**, 625–635.
26. Davis,E.J., Lachaud,C., Appleton,P., Macartney,T.J., Nathke,I. and Rouse,J. (2012) DVC1 (C1orf124) recruits the p97 protein segregase to sites of DNA damage. *Nat. Struct. Mol. Biol.*, **19**, 1093–1100.
27. Juhasz,S., Balogh,D., Hajdu,I., Burkovics,P., Villamil,M.A., Zhuang,Z. and Haracska,L. (2012) Characterization of human Spartan/C1orf124, an ubiquitin-PCNA interacting regulator of DNA damage tolerance. *Nucleic Acids Res.*, **40**, 10795–10808.
28. Machida,Y., Kim,M.S. and Machida,Y.J. (2012) Spartan/C1orf124 is important to prevent UV-induced mutagenesis. *Cell Cycle*, **11**, 3395–3402.
29. Mosbech,A., Gibbs-Seymour,I., Kagias,K., Thorslund,T., Beli,P., Povlsen,L., Nielsen,S.V., Smedegaard,S., Sedgwick,G., Lukas,C. *et al.* (2012) DVC1 (C1orf124) is a DNA damage-targeting p97 adaptor that promotes ubiquitin-dependent responses to replication blocks. *Nat. Struct. Mol. Biol.*, **19**, 1084–1092.
30. Day,T.A., Palle,K., Barkley,L.R., Kakusho,N., Zou,Y., Tateishi,S., Verreault,A., Masai,H. and Vaziri,C. (2010) Phosphorylated Rad18 directs DNA polymerase eta to sites of stalled replication. *J. Cell Biol.*, **191**, 953–966.
31. Watanabe,K., Tateishi,S., Kawasuji,M., Tsurimoto,T., Inoue,H. and Yamaizumi,M. (2004) Rad18 guides poleta to replication stalling sites through physical interaction and PCNA monoubiquitination. *EMBO J.*, **23**, 3886–3896.
32. Barkley,L.R., Palle,K., Durando,M., Day,T.A., Gurkar,A., Kakusho,N., Li,J., Masai,H. and Vaziri,C. (2012) c-Jun N-terminal kinase-mediated Rad18 phosphorylation facilitates Poleta recruitment to stalled replication forks. *Mol. Biol. Cell*, **23**, 1943–1954.
33. Maher,V.M., McCormick,J.J., Grover,P.L. and Sims,P. (1977) Effect of DNA repair on the cytotoxicity and mutagenicity of polycyclic hydrocarbon derivatives in normal and xeroderma pigmentosum human fibroblasts. *Mutat. Res.*, **43**, 117–138.
34. Maher,V.M., Ouellette,L.M., Mittlestat,M. and McCormick,J.J. (1975) Synergistic effect of caffeine on the cytotoxicity of ultraviolet irradiation and of hydrocarbon epoxides in strains of Xeroderma pigmentosum. *Nature*, **258**, 760–763.
35. Pavlov,Y.I., Nguyen,D. and Kunkel,T.A. (2001) Mutator effects of overproducing DNA polymerase eta (Rad30) and its catalytically inactive variant in yeast. *Mutat. Res.*, **478**, 129–139.
36. Ito,W., Yokoi,M., Sakayoshi,N., Sakurai,Y., Akagi,J.I., Mitani,H. and Hanaoka,F. (2012) Stalled Polη at its cognate substrate initiates an alternative translesion synthesis pathway via interaction with REV1. *Genes Cells*, **17**, 98–108.
37. Johnson,R.E., Kondratick,C.M., Prakash,S. and Prakash,L. (1999) hRAD30 mutations in the variant form of xeroderma pigmentosum. *Science*, **285**, 263–265.

38. Pawsey,S.A., Magnus,I.A., Ramsay,C.A., Benson,P.F. and Giannelli,F. (1979) Clinical, genetic and DNA repair studies on a consecutive series of patients with xeroderma pigmentosum. *Q. J. Med.*, **48**, 179–210.
39. Shiomi,N., Mori,M., Tsuji,H., Imai,T., Inoue,H., Tateishi,S., Yamaizumi,M. and Shiomi,T. (2007) Human RAD18 is involved in S phase-specific single-strand break repair without PCNA monoubiquitination. *Nucleic Acids Res.*, **35**, e9.
40. Biertumpfel,C., Zhao,Y., Kondo,Y., Ramon-Maiques,S., Gregory,M., Lee,J.Y., Masutani,C., Lehmann,A.R., Hanaoka,F. and Yang,W. (2010) Structure and mechanism of human DNA polymerase eta. *Nature*, **465**, 1044–1048.
41. Bi,X., Barkley,L.R., Slater,D.M., Tateishi,S., Yamaizumi,M., Ohmori,H. and Vaziri,C. (2006) Rad18 regulates DNA polymerase kappa and is required for recovery from S-phase checkpoint-mediated arrest. *Mol. Cell. Biol.*, **26**, 3527–3540.
42. Cimprich,K.A. and Cortez,D. (2008) ATR: an essential regulator of genome integrity. *Nat. Rev. Mol. Cell Biol.*, **9**, 616–627.
43. Zou,L. and Elledge,S.J. (2003) Sensing DNA damage through ATRIP recognition of RPA-ssDNA complexes. *Science*, **300**, 1542–1548.
44. Huang,T.T., Nijman,S.M., Mirchandani,K.D., Galardy,P.J., Cohn,M.A., Haas,W., Gygi,S.P., Ploegh,H.L., Bernards,R. and D'Andrea,A.D. (2006) Regulation of monoubiquitinated PCNA by DUB autocleavage. *Nat. Cell Biol.*, **8**, 339–347.
45. Broughton,B.C., Cordonnier,A., Kleijer,W.J., Jaspers,N.G., Fawcett,H., Raams,A., Garritsen,V.H., Stary,A., Avril,M.F., Boudsocq,F. *et al.* (2002) Molecular analysis of mutations in DNA polymerase eta in xeroderma pigmentosum-variant patients. *Proc. Natl Acad. Sci. USA*, **99**, 815–820.
46. Tanioka,M., Masaki,T., Ono,R., Nagano,T., Otoshi-Honda,E., Matsumura,Y., Takigawa,M., Inui,H., Miyachi,Y., Moriwaki,S. *et al.* (2007) Molecular analysis of DNA polymerase eta gene in Japanese patients diagnosed as xeroderma pigmentosum variant type. *J. Invest. Dermatol.*, **127**, 1745–1751.
47. Haracska,L., Johnson,R.E., Unk,I., Phillips,B., Hurwitz,J., Prakash,L. and Prakash,S. (2001) Physical and functional interactions of human DNA polymerase eta with PCNA. *Mol. Cell Biol.*, **21**, 7199–7206.
48. Masutani,C., Araki,M., Yamada,A., Kusumoto,R., Nogimori,T., Maekawa,T., Iwai,S. and Hanaoka,F. (1999) Xeroderma pigmentosum variant (XP-V) correcting protein from HeLa cells has a thymine dimer bypass DNA polymerase activity. *EMBO J.*, **18**, 3491–3501.
49. Hishiki,A., Hashimoto,H., Hanafusa,T., Kamei,K., Ohashi,E., Shimizu,T., Ohmori,H. and Sato,M. (2009) Structural basis for novel interactions between human translesion synthesis polymerases and proliferating cell nuclear antigen. *J. Biol. Chem.*, **284**, 10552–10560.
50. Kannouche,P., Fernandez de Henestrosa,A.R., Coull,B., Vidal,A.E., Gray,C., Zicha,D., Woodgate,R. and Lehmann,A.R. (2002) Localization of DNA polymerases eta and iota to the replication machinery is tightly co-ordinated in human cells. *EMBO J.*, **21**, 6246–6256.
51. Sabbioneda,S., Gourdin,A.M., Green,C.M., Zotter,A., Giglia-Mari,G., Houtsmuller,A., Vermeulen,W. and Lehmann,A.R. (2008) Effect of proliferating cell nuclear antigen ubiquitination and chromatin structure on the dynamic properties of the Y-family DNA polymerases. *Mol. Biol. Cell*, **19**, 5193–5202.
52. Liu,G. and Chen,X. (2006) DNA polymerase eta, the product of the xeroderma pigmentosum variant gene and a target of p53, modulates the DNA damage checkpoint and p53 activation. *Mol. Cell Biol.*, **26**, 1398–1413.
53. Wani,M.A., Zhu,Q.Z., El-Mahdy,M. and Wani,A.A. (1999) Influence of p53 tumor suppressor protein on bias of DNA repair and apoptotic response in human cells. *Carcinogenesis*, **20**, 765–772.
54. Laposa,R.R., Feeney,L., Crowley,E., de Feraudy,S. and Cleaver,J.E. (2007) p53 suppression overwhelms DNA polymerase eta deficiency in determining the cellular UV DNA damage response. *DNA Repair (Amst)*, **6**, 1794–1804.
55. Tomida,J., Masuda,Y., Hiroaki,H., Ishikawa,T., Song,I., Tsurimoto,T., Tateishi,S., Shiomi,T., Kamei,Y., Kim,J. *et al.* (2008) DNA damage-induced ubiquitylation of RFC2 subunit of replication factor C complex. *J. Biol. Chem.*, **283**, 9071–9079.
56. Tissier,A., Kannouche,P., Reck,M.P., Lehmann,A.R., Fuchs,R.P. and Cordonnier,A. (2004) Co-localization in replication foci and interaction of human Y-family members, DNA polymerase pol eta and REVl protein. *DNA Repair (Amst)*, **3**, 1503–1514.
57. Yanagihara,H., Kobayashi,J., Tateishi,S., Kato,A., Matsuura,S., Tauchi,H., Yamada,K., Takezawa,J., Sugasawa,K., Masutani,C. *et al.* (2011) NBS1 recruits RAD18 via a RAD6-like domain and regulates Pol eta-dependent translesion DNA synthesis. *Mol. Cell*, **43**, 788–797.
58. Yang,X.H., Shiotani,B., Classon,M. and Zou,L. (2008) Chk1 and Claspin potentiate PCNA ubiquitination. *Genes Dev.*, **22**, 1147–1152.
59. Temviriyanukul,P., Meijers,M., van Hees-Stuivenberg,S., Boei,J.J., Delbos,F., Ohmori,H., de Wind,N. and Jansen,J.G. (2012) Different sets of translesion synthesis DNA polymerases protect from genome instability induced by distinct food-derived genotoxins. *Toxicol. Sci.*, **127**, 130–138.
60. Lange,S.S., Takata,K. and Wood,R.D. (2011) DNA polymerases and cancer. *Nat. Rev. Cancer*, **11**, 96–110.
61. Jung,Y.S., Liu,G. and Chen,X. (2010) Pirh2 E3 ubiquitin ligase targets DNA polymerase eta for 20S proteasomal degradation. *Mol. Cell Biol.*, **30**, 1041–1048.
62. Jung,Y.S., Qian,Y. and Chen,X. (2012) DNA polymerase eta is targeted by Mdm2 for polyubiquitination and proteasomal degradation in response to ultraviolet irradiation. *DNA Repair (Amst)*, **11**, 177–184.
63. Skoneczna,A., McIntyre,J., Skoneczny,M., Policinska,Z. and Sledziewska-Gojska,E. (2007) Polymerase eta is a short-lived, proteasomally degraded protein that is temporarily stabilized following UV irradiation in Saccharomyces cerevisiae. *J. Mol. Biol.*, **366**, 1074–1086.
64. Jung,Y.S., Hakem,A., Hakem,R. and Chen,X. (2011) Pirh2 E3 ubiquitin ligase monoubiquitinates DNA polymerase eta to suppress translesion DNA synthesis. *Mol. Cell Biol.*, **31**, 3997–4006.

—Original—

An Extended Family with Familial Medullary Thyroid Carcinoma and Hirschsprung's Disease

Takehito Igarashi[1], Ritsuko Okamura[1], Tomoo Jikuzono[1], Shinya Uchino[2], Iwao Sugitani[1] and Kazuo Shimizu[1]

[1]Division of Endocrine Surgery, Department of Surgery, Nippon Medical School
[2]Department of Surgery, Noguchi Hospital

Abstract

Familial medullary thyroid carcinoma (FMTC) is an autosomal dominant inherited disease that has highly characteristic clinical features, including medullary thyroid carcinoma (MTC). Mutation of the *RET* proto-oncogene is known to be responsible for development of FMTC and for multiple endocrine neoplasia types 2A and 2B. Hirschsprung's disease is the most common form of structural intestinal obstructive disease in human newborns. Hirschsprung's disease is defined by the absence of neural crest-derived enteric ganglia along a variable length of the bowel that invariably involves the rectoanal junction. Co-segregation of FMTC and Hirschsprung's disease is uncommon; nevertheless, in 3 generations of 1 family, we observed 5 patients with FMTC, 2 patients with Hirschsprung's disease, and 1 patient with characteristics of both FMTC and Hirschsprung's disease. Moreover, a Cys620Ser mutation in *RET* was identified in 4 of the 8 patients. This mutation had both activating and inactivating effects on the RET (REarranged during Transfection) protein. There were individual differences in the penetrance of Hirschsprung's disease due to the *RET* mutation, but the penetrance of MTC was uniform and high. Genetic testing is important for making decisions about treatment and follow-up in families of this kind.
(J Nippon Med Sch 2014; 81: 64–69)

Key words: familial medullary thyroid carcinoma, Hirschsprung's disease, *RET*

Introduction

Hereditary medullary thyroid carcinoma (MTC) is autosomal dominant inherited disease and occurs in multiple endocrine neoplasia type 2A (MEN2A) and type 2B (MEN2B), as well as in familial MTC (FMTC). Each of these diseases has been associated with activating mutations of the *RET* proto-oncogene[1,2]. Several *RET* mutations cause activation of the *RET* gene and facilitate cellular signal transduction[3,4].

The most common germ-line mutations involve the extracellular domain of *RET* at codons 609, 611, 618, 620, 630, and 634[5–8]. Mutations occur in the tyrosine kinase domain of *RET* at codons 768, 790, 791, 804, and 891[5–8].

Hirschsprung's disease is the most common type

Correspondence to Takehito Igarashi, MD, PhD, Division of Endocrine Surgery, Department of Surgery, Nippon Medical School, 1–1–5 Sendagi, Bunkyo-ku, Tokyo 113–8603, Japan
E-mail: takehito@nms.ac.jp
Journal Website (http://www.nms.ac.jp/jnms/)

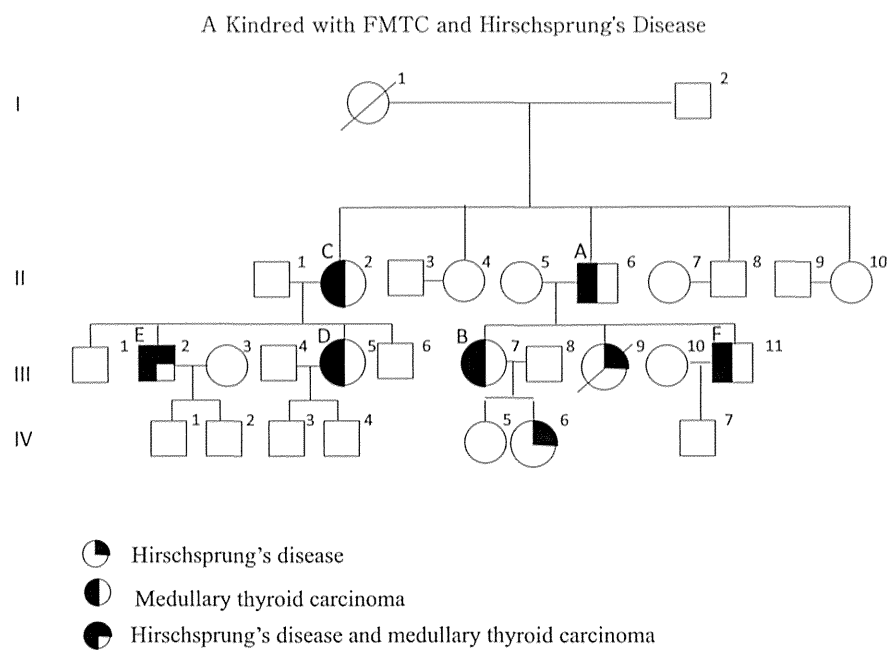

Fig. 1 The pedigree of the described family.
Three patients presented with MTC, 3 patients presented with Hirschsprung's disease, and 1 presented with concomitant MTC and Hirschsprung's disease; each patient is indicated in this pedigree. Two patients presented with Hirschsprung's disease but did not undergo genetic testing.

of structural intestinal obstructive disease in human newborns. It is characterized by the absence of neural crest-derived enteric ganglia along a variable length of the bowel that invariably includes the rectoanal junction. Hirschsprung's disease is associated with various chromosomal abnormalities and inherited disorders. The major susceptibility gene is *RET*, and *RET* mutations have been identified in 50% of familial cases and 15% to 35% of sporadic cases of Hirschsprung's disease[12].

The *RET* proto-oncogene, which is critical to the development of MTC and of Hirschsprung's disease, encodes RET (REarranged during Transfection), a transmembrane receptor-type kinase that is expressed in cells derived from the neural crest and the urogenital tract.

A single *RET* mutation rarely causes both activation and inactivation of RET signaling. Reportedly, the *RET* gene is deeply involved in the development of MEN2, FMTC, and Hirschsprung's disease[5-7]. The clinical severities of Hirschsprung's disease due to different *RET* mutations are highly individual and, as a result, show incomplete penetrance (~50%). Therefore, only affected persons in whom MTC develops are recognized in family pedigrees of these diseases. We examined data from an extended family in which Hirschsprung's disease, MTC, and 1 case of concomitant Hirschsprung's disease and MTC were evident; notably, a codon 620 *RET* mutation was segregating in this family.

Materials and Methods

This study was retrospective, and each patient gave written informed consent to participate. Data were extracted from medical records; additional medical interviews and laboratory examinations were also conducted. Genetic tests were performed following an independent review by the Institutional Independent Review Board and according to national guidelines. Subjects were free to withdraw from the study at any time. Interviews about the presence of the diseases in the family were conducted, and a pedigree was created.

Summary of Patients (Fig. 1)

Patient A (II-6): A 57-year-old man presented with neck swelling during a medical check-up and asked us to investigate it. Close inspection resulted in the diagnosis of MTC. The family history revealed a

Table 1 Overview of preoperative data

Patient	Age at operation (years)	Sex	Calcitonin (pg/mL)	Carcinoembryonic antigen (ng/mL)	*RET* mutation
A (II-6)	57	M	670	8.5	620 TGC to TCC
B (III-7)	33	F	32	0.6	620 TGC to TCC
C (II-2)	64	F	390	10.7	Testing not done
D (III-5)	33	F	340	23.6	Testing not done
E (III-2)	40	M	733	5.1	620 TGC to TCC
F (III-11)	33	M	1,134	6.2	620 TGC to TCC

daughter (III-9) who had died of Hirschsprung's disease as an infant, and a grandchild who had been treated for Hirschsprung's disease. Additionally, his older sister had undergone right lobectomy of the thyroid because of MTC. Therefore, we concluded that the MTC in patient A was not sporadic but familial. We recommend genetic testing, and the patient agreed. His siblings were screened (the value of carcinoembryonic antigen [CEA] and calcitonin were determined, and the thyroid glands were evaluated with ultrasonography) at the same time, and no abnormalities were found other than a mass in the residual thyroid gland in an older sister.

Patient B (III-7): A 33-year-old woman whose daughter (IV-6) had been treated for Hirschsprung's disease agreed to undergo genetic testing. She had no thyroid symptoms, but she wanted to undergo prophylactic total thyroidectomy because of an *RET* mutation.

Patient C (II-2): A 64-year-old woman was found to have recurrent MTC in the residual thyroid gland; she decided to undergo complementary total thyroidectomy but refused genetic testing.

Patient D (III-5): A 33-year-old woman was worried about increased levels of CEA after surgery for breast cancer and visited our hospital. She was found to have MTC but refused genetic testing.

Patient E (III-2): A 40-year-old man, whose mother and young sister had undergone operations for MTC, had undergone 4 different colorectal operations as a child because of Hirschsprung's disease; he consulted another hospital, where MTC was diagnosed, and agreed to undergo genetic testing.

Patient F (III-11): A 33-year-old man wanted to have the thyroid checked because his father and sister had undergone surgery for MTC. After close inspection, he was also found to have MTC and agreed to undergo genetic testing.

Preoperative values of CEA and calcitonin for each of these patients are shown in **Table 1**.

Gene Analysis

A DNA extractor WB kit (Wako Pure Chemical Industries, Ltd., Osaka, Japan) was used according to the manufacturer's instructions to extract genomic DNA from samples of peripheral blood. The absorbance at 260 nm was determined with a spectrophotometer (SmartSpec 3000, Bio-Rad Laboratories, Inc., Hercules, CA, USA) to measure the DNA concentration in each sample of genomic DNA.

Exons 10, 11, and 13–16 of *RET* were amplified from genomic DNA from patient A via the polymerase chain reaction (PCR); previously published primers and PCR conditions were used[8]. A mutation was discovered in exon 10 in genomic DNA from patient A, and all subsequent analyses of *RET* in DNA samples from this family were restricted to exon 10.

Amplified PCR fragments were purified with a purification kit (QIAquick PCR Purification Kit, Qiagen, Hilden, Germany) and subjected to additional PCR with sense or antisense primers and reaction mix (ABI PRISM Big Dye Terminator v1.1 Cycle Sequencing Ready Reaction mix, Applied Biosystems, Foster City, CA, USA). Each sample containing resultant PCR products was eluted through a spin column (Centri-Sep, Applied Biosystems), and the PCR products were sequenced on an automated capillary DNA sequencer (ABI PRISM 3100, Applied Biosystems).

Table 2 Overview of operative findings

Patient	Operation	Time (min)	Postoperative diagnosis
A (II-6)	Total thyroidectomy+D3a	168	pT1(m), pN1b, pEx0
B (III-7)	Total thyroidectomy+CND	94	pT1(m), pN0, pEx0
C (II-2)	Total thyroidectomy+D3a	65	pT2(m), pN0, pEx0
D (III-5)	Total thyroidectomy+D3a	230	pT1(m), pN0, pEx0
E (III-2)	Total thyroidectomy+CND	107	pT1, pN1a, pEx0
F (III-11)	Total thyroidectomy+CND	70	pT1(m), pN0, pEx0

D3a, bilateral lateral lymph node dissection; CND, central lymph node dissection

Results

In this extended family, 6 persons were found to have MTC and underwent surgery. Four of the 6 were found to carry a Cys620Ser mutation of *RET*. Each surgery was performed without incident and resulted in a successful outcome (**Table 2**). None of the patients had recurrent laryngeal nerve palsy or hypoparathyroidism. The recovery period for patient F has been too short to reliably evaluate the outcome, as he underwent the operation only 2 months ago as of this writing. More than 5 years have passed since surgery for the other patients with MTC, and none have shown any evidence of recurrence; however, the CEA and calcitonin levels in patient C remain high.

Three patients with Hirschsprung's disease were identified, but 2 of them did not undergo genetic testing (**Fig. 1**, **Table 1**). One of these patients presented with concomitant FMTC and Hirschsprung's disease and carried the Cys620Ser mutation of *RET*.

It is extremely important to carefully monitor the course of each patient over the long term. Four of the 6 patients in the present family were found to have an *RET* mutation that could account for the disease. In each of these patients DNA sequencing revealed a Cys620Ser mutation of the *RET* gene (**Table 1**).

Because we did not obtain parental consent, we did not perform genetics tests of samples from a daughter of patient B. However, the daughter has never had a mass of the thyroid gland or elevated serum levels of calcitonin or CEA. Our analysis of this family suggests that patient B's daughter should also be followed up carefully because, on the basis on the family history, MTC is expected to develop.

Discussion

Co-segregation of FMTC and Hirschsprung's disease is uncommon, but in 1 extended family we observed 5 patients with FMTC, 3 patients with Hirschsprung's disease, and 1 patient who showed characteristics of both FMTC and Hirschsprung's disease. Co-segregation of FMTC and Hirschsprung's disease relates mostly to the cysteine-rich area at codon 620 of *RET*. All of the patients were related to one another, and 4 of them were found to carry the same *RET* allele, Cys620Ser.

Codon 620 of *RET* has been called the "Janus gene" because, like the Roman god of doorways, it can face in both directions; RET gain-of-function mutation causes MTC, and RET loss-of-function mutation causes Hirschsprung's disease.

RET is important for cellular growth and differentiation and is involved in several types of multiple neoplasia, such as MEN2A, MEN2B, and FMTC[1,2]. Activation patterns of a number of *RET* mutations have been reported to be associated with certain types of disease[3,4]. Several large-scale studies have demonstrated a correlation between *RET* mutations and disease phenotypes[14]. The Cys634Arg mutation results in MEN2A, and Met918Thr results in self-dimerization and constitutive RET activation, leading to abnormal cell growth and dysfunction of differentiation[5–7]. These findings indicate that RET activation is responsible for the pathogenesis of these diseases.

Hirschsprung's disease is one of the most common diseases caused by malformation of neural crest-

derived enteric structures in neonates led by dysfunction of RET. Butter *et al.* have reported on 20 patients with Hirschsprung's disease who each carried a mutation of *RET*; each patient also underwent prophylactic thyroidectomy and was ultimately healthy and cancer-free[9]. Hirschsprung's disease is rarely reported with other neoplastic diseases. Patients with Hirschsprung's disease and MTC have been reported in a single family[10]; however, co-segregation of FMTC and Hirschsprung's disease is rare.

Here, 4 persons with a mutation in codon 620 of *RET* gene were found in a single family, but how this mutation could result in the diseases observed in each individual is difficult to understand.

The biological effects of codon 620 of *RET* have been studied to understand RET gain-of-function mutations and the development of MTC and to understand RET loss-of-function mutations and the development of Hirschsprung's disease.

Several studies have demonstrated that the cysteine mutations in the extracellular domain activate RET by inducing covalent RET dimerization[13]. This molecular mechanism could account for RET gain-of-function mutations[11,13].

Codon 620 *RET* mutation decreases expression of the cell-surface form of RET protein. These mutations appear to impair the transport of RET to the plasma membrane or the proper maturation of RET[13].

The RET protein and glial cell line-derived neurotrophic factor family (GDNF) receptor α1 (GFRα1) form a signaling receptor complex for GDNF. In particular, signaling by GDNF promotes the survival of dopaminergic neurons. Arighi *et al.*[11] have demonstrated that cells carrying a mutation in codon 620 of *RET* are unable to migrate and branch in response to GDNF. Moreover, insensitivity to GDNF renders cells more prone to apoptosis. These features are considered to be loss-of-function phenotypes[11].

Whole-gene analyses of *RET*, gene-expression profiling, and whole-genome sequencing can be useful for revealing the disease mechanisms and the signal transduction pathway of RET. The results of the present study suggest that sequencing of *RET* should be performed in cases of FMTC or Hirschsprung's disease and in high-risk carriers with a hereditary background as a clinical guideline for FMTC, Hirschsprung's disease, and MEN2[14].

Conflict of Interest: None of the authors have any potential conflicts of interest associated with this research.

References

1. Hofsttra RM, Lansvater RM, Ceccheri I, Stlup RP, Stelwagen T, et al.: A mutation in the RET proto-oncogene associated with multiple endocrine type 2B and sporadic medullary thyroid carcinoma. Nature 1994; 367: 375–376.
2. Raue F, Frank-Raue K: Genotype-phenotype relationship in multiple endocrine neoplasia type 2 Implication for clinical management. Horomones (Athens) 2009; 8: 23–28.
3. Santoro M, Carlomagno F, Romano A, Bottaro DP, Dathan NA, et al.: Activation RET as a dominant transforming gene by germ line mutations of MEN2A and MEN2B. Science 1995; 267: 381–383.
4. Berndt I, Reuter M, Saller B, et al.: A new hot spot for mutation the ret proto-oncogene causing familial medullary thyroid carcinoma and multiple endocrine neoplasia type 2A. J Clin Endocrinol Metab 1998; 83: 770–774.
5. Mulligan LM, Eng C, Healy CS, Clayton D, Kwok JB, et al.: Specific mutations of RET proto-oncogene are related to disease phenotype in MEN 2A and FMTC. Nat Genet 1994; 6: 70–74.
6. Romei C, Elisei R, Prinhera A, Coccherini I, Mancusi F, et al.: Somatic mutations of the ret proto-oncogene in sporadic medullary thyroid carcinoma are not restricted to exon 16 and are associated with tumor recurrence. J Clin Endocrinol Metab 1996; 81: 1619–1622.
7. Schuffenecker I, Virally-Mond M, Brohet R, Goldgar D, Conte-Devol B, et al.: Risk and penetrance of primary hyperparathyroidism in multiple endocrine neoplasia type 2A families with mutations at codon 364 of the RET proto-oncogene; Groupe D'etude des Tumeurs aCalcitonine. J Clin Endocrinol Metab 1998; 83: 487–491.
8. Uchino S, Noguchi S, Adachi M, Sato M, Yamashita H, et al.: Novel point mutations and allele loss at the RET locus in sporadic medullary thyroid carcinomas. Jpn J Cancer Res 1998; 89: 411–418.
9. Butter A, Gangnel J, Al-Jazaeri A, Emran MA, Deal C, et al.: Prophylactic thydoidectomy in pediatric carries of multiple endocrine neoplasia type2A or familial medullary thyroid carcinoma: mutation in C 620 is associated with Hirschspung's disease. J Pediatr Surg 2007; 2: 203–206.
10. Fialkowski EA, DABenedetti MK, Moley JF, Bachrach B: RET proto-oncogene testing in infants presenting with Hirschsprung disease indentifies 2 new multiple neoplasia 2a in kidreds. J Pediatr Surg

2008; 43: 188–190.
11. Arighi E, Posueva A, Degl'innocenti D, Borrello MG, Carniti C, et al.: Biological effect of the dual phenotypic Janus mutation or ret segregating both multiple endocrine neoplasia type 2 and Hirschsprung's disease. Mol Endocrinol 2004; 18: 1004–1017.
12. Amiel J, Lyonnet S: Hirschsprung disease, associated syndromes, and genetics: a review. J Med Genet 2001; 38: 729–739.
13. Ito S, Iwashita T, Asai N, Murakami H, Iwata Y, et al.: Biological Properties of Ret with Cysteine Mutation Correlate with Mutiple Endocrine Neoplasia Type 2A, Familial Medullary Thyroid Carcinoma, and Hirschsprung's Disease Phenotype. CANCER RESEARCH 1997; 57: 2870–2872.
14. American Thyroid Association Guideline Task Force: Medullary thyroid cancer: management guidelines of the American Thyroid Association. Thyroid 2009; 19: 565–612.

(Received, June 14, 2013)
(Accepted, July 17, 2013)

J Clin Immunol
DOI 10.1007/s10875-014-0058-8

BRIEF COMMUNICATION

A Complement Factor B Mutation in a Large Kindred with Atypical Hemolytic Uremic Syndrome

Michinori Funato · Osamu Uemura · Katsumi Ushijima · Hidenori Ohnishi · Kenji Orii · Zenichiro Kato · Satoshi Yamakawa · Takuhito Nagai · Osamu Ohara · Hideo Kaneko · Naomi Kondo

Received: 9 July 2013 / Accepted: 15 May 2014

Abstract
Purpose Gain-of-function mutations in complement factor B (*CFB*) were recently identified in patients with atypical hemolytic uremic syndrome (aHUS), but are extremely rare. Our purpose is to describe a large kindred with aHUS associated with a *CFB* mutation and to further understand *CFB*-mutated aHUS patients.
Methods and Results We report a large kindred in which 3 members had aHUS. This kindred revealed that 9 of 12 members, including 2 affected patients, had persistent activation of the alternative pathway with low complement component 3 and that those 9 members showed a *CFB* mutation (c.1050G>C, p.Lys350Asn) in exon 8. This missense mutation was heterozygous in 8 of them and homozygous in only one. From structural studies, this mutation is shown to be located in close proximity to the Mg^2-binding site within a von Willebrand factor type A domain of CFB, resulting in a gain-of-function effect of CFB and predisposition to aHUS. At present, 2 of the 3 members with aHUS have maintained normal renal function for a long-term period.
Conclusions This kindred illustrates that a *CFB* mutation (c.1050G>C, p.Lys350Asn) can result in aHUS. In the future, phenotype-genotype correlations and outcome in *CFB*-mutated aHUS patients need to be further investigated by accumulation of a number of cases.

Keywords Atypical hemolytic uremic syndrome · complement alternative pathway · complement factor B · gain-of-function · large kindred

Abbreviations

aHUS	Atypical hemolytic uremic syndrome
CFH	Complement factor H
CFI	Complement factor I
MCP	Membrane cofactor protein
CFB	Complement factor B
C3	Complement component 3
THBD	Thrombomodulin
VWA	von Willebrand factor type A
SP	Serine protease

Introduction

Atypical hemolytic uremic syndrome (aHUS) is known to be a disorder of the regulation of the complement alternative pathway, and is also broadly interpreted as a primary immunodeficiency

Electronic supplementary material The online version of this article (doi:10.1007/s10875-014-0058-8) contains supplementary material, which is available to authorized users.

M. Funato (✉) · H. Ohnishi · K. Orii · Z. Kato · N. Kondo
Department of Pediatrics, Graduate School of Medicine, Gifu University, 1-1 Yanagido, Gifu 501-1194, Japan
e-mail: mfunato@me.com

M. Funato · H. Kaneko
Department of Clinical Research, National Hospital Organization, Nagara Medical Center, Gifu, Japan

O. Uemura · S. Yamakawa · T. Nagai
Department of Pediatric Nephrology, Aichi Children's Health and Medical Center, Obu, Japan

K. Ushijima
Department of Pediatrics, Yokkaichi Municipal Hospital, Yokkaichi, Japan

O. Ohara
Laboratory for Immunogenomics, RIKEN Research Center for Allergy and Immunology, Yokohama, Japan

O. Ohara
Department of Human Genome Research, Kazusa DNA Research Institute, Kisarazu, Japan

Published online: 08 June 2014